OPEN ACCESS

Klimarealistene
P.O. Box 33,
3901 Porsgrunn
Norway
ISSN: 2703-9072

Correspondence:
roy.clark@ventu-raphotonics.com

Vol. 3.5 (2023)

pp. 421-444

Time Dependent Climate Energy Transfer: The Forgotten Legacy of Joseph Fourier

Roy Clark

Ventura Photonics,
Thousand Oaks, CA, USA

Abstract

Joseph Fourier discussed the temperature of the earth in two similar memoires (reviews) in 1824 and 1827. An important and long neglected part of this work is his description of the time dependence of the surface energy transfer. In particular, he was able to explain the seasonal time delays or phase shifts between the peak solar flux and the subsurface temperature response using his theory of heat published in 1822. This is clear evidence for a non-equilibrium thermal response to the solar flux. Diurnal and seasonal phase shifts occur in both the ocean and land temperature records. These phase shifts provide important additional information about the time dependent energy transfer processes that determine the surface temperature. Unfortunately, starting with the work of Pouillet in 1836, this time dependence was neglected and replaced by an equilibrium average climate. It was assumed, incorrectly, that the surface temperature could be determined using average values for just the solar and IR flux terms. This approach created CO_2 induced global warming as a mathematical artifact in the simplistic equilibrium air column model used by Arrhenius in 1896. Physical reality was abandoned in favor of mathematical simplicity. The equilibrium assumption is still the foundation of the fraudulent climate models in use today. In order to move beyond the pseudoscience of radiative forcings, feedbacks and climate sensitivity to CO_2 it is necessary to follow Fourier and restore the time dependence to the surface energy transfer. A change in flux produces a change in the rate of cooling (or heating) of a thermal reservoir, not a change in temperature.

Keywords: Convection Transition Temperature; Diurnal Phase Shift; Exchange Energy; Joseph Fourier; Ocean-Land Temperature Coupling; Phase Shift; Seasonal Phase Shift; Thermal Equilibrium; Time Dependent Energy Transfer.

Submitted 2023-11-20, Accepted 2023-12-02. https://doi.org/10.53234/scc202310/25

1. Introduction

The term ‘equilibrium’ is often used incorrectly in climate science. The concept of radiative equilibrium was introduced by Kirchoff (1860):

At thermal equilibrium, the power radiated by an object must be equal to the power absorbed.

The lunar surface under solar illumination is close to thermal equilibrium. The absorbed solar flux is emitted back to space as LWIR radiation with almost no time delay. At the lunar equator, the maximum surface temperature at lunar noon is near 390 K (117 °C). As the solar flux changes, the surface temperature changes so that the emitted LWIR flux matches the absorbed solar flux, Clark and Rörsch (2023). The term equilibrium as used by Arrhenius, (1896) was not a radiative equilibrium, it was simply a mathematical equality between an average absorbed solar flux and an average emitted LWIR flux. Similarly, the term equilibrium used by Manabe and Wetherald, (1967) was a steady state condition. The average solar and LWIR fluxes in and out of the model were equal and the internal air layer and surface temperatures were stable. The temperature change during each model time step was very small. Such a condition is not found in the earth’s atmosphere.

An important property of a non-equilibrium thermal system is the time delay or phase shift between the time varying heat source and the temperature response of the thermal reservoir. Joseph Fourier discussed the temperature of the earth in two similar memoires in 1824 and 1827, Fourier (1824; 1827). He correctly described the time dependent heating of the earth's land surface by the solar flux using his theory of heat, Fourier (1822). He also described ocean solar heating and atmospheric cooling by convection. However, he did not use the term 'greenhouse effect'. Instead, he described a solar calorimeter with glass windows. An important part of his work was the description of the seasonal time delay or phase shift in the subsurface heat transfer.

> *At a moderate depth; as three or four meters, the temperature observed does not vary during each day, but the change is very perceptible in the course of a year, it varies and falls alternately. The extent of these variations, that is, the difference between the maximum and minimum of temperature, is not the same at all depths, it is inversely as the distance from the surface. The different points of the same vertical line do not arrive at the same time at the extreme temperatures. ..... The results observed are in accordance with those furnished by the theory, no phenomenon is more completely explained.* *Fourier 1824, p. 144.*

This is indisputable evidence for a non-equilibrium thermal response to the solar flux. There is a time delay as heat flows in and out of the ground or the oceans. Such seasonal and diurnal phase shifts have been ignored in climate science for almost 200 years. Similar phase shifts occur in other energy storage devices including capacitors in AC electronic circuits and in optical passive cavity resonators (cavity ringdown), Clark (1993).

The phase shifts provide important additional information about the time dependent energy transfer processes that determine the surface temperature. Unfortunately, starting with the work of Pouillet (1836), this time dependence was neglected and it was incorrectly assumed the surface temperature could be determined using average values for just the solar and IR flux terms. Physical reality was abandoned in favor of mathematical simplicity. Arrhenius (1896) stated:

> *III.* ***Thermal Equilibrium*** *on the Surface and in the Atmosphere of the Earth*
>
> *All authors agree in the view that there prevails an* ***equilibrium*** *in the temperature of the earth and of its atmosphere.* *Arrhenius 1896, p. 254.*

Manabe and Wetherald (1967) set out to answer the following questions:

> *1) How long does it take to reach a state of* ***thermal equilibrium*** *when the atmosphere maintains a realistic distribution of relative humidity that is invariant with time?*
>
> *2) What is the influence of various factors such as the solar constant, cloudiness, surface albedo and the distributions of various atmospheric absorbers on the* ***equilibrium temperature*** *of the atmosphere with a realistic distribution of relative humidity?*
>
> *3) What is the* ***equilibrium temperature*** *of the earth's surface corresponding to realistic values of these factors?* *Manabe and Wetherald, 1967, p. 242.*

Knutti and Hegerl, (2008) stated:

> *When the radiation balance of the Earth is perturbed, the global surface temperature will warm and adjust to a* ***new equilibrium state****.* *Knutti and Hegerl, 2008, p. 735.*

Manabe and Wetherald, (1967) copied Arrhenius and created the equilibrium climate fantasy land in which the climate modelers play their computer games with radiative forcings, feedbacks and a climate sensitivity to CO_2. This fantasy land is described in Chapter 7 of the Working Group 1 IPCC Climate Assessment Report (2021):

> *This chapter assesses the present state of knowledge of Earth's energy budget, that is, the main flows of energy into and out of the Earth system, and how these energy flows govern the climate response to a radiative forcing. Changes in atmospheric composition and land use, like those caused by anthropogenic greenhouse gas emissions and emissions of aerosols and their precursors, affect climate through perturbations to Earth's top-of-atmosphere energy budget. The effective radiative forcings (ERFs) quantify these perturbations, including any consequent adjustment to the climate system (but excluding surface temperature response). How the climate system responds to a given forcing is determined by climate feedbacks associated with physical, biogeophysical and biogeochemical processes. These feedback processes are assessed, as are useful measures of global climate response, namely* ***equilibrium climate sensitivity*** *(ECS) and the transient climate response (TCR).*

There is no climate equilibrium state that can be perturbed by an increase in the atmospheric concentration of CO_2 or other greenhouse gases. In the time step integration algorithm used by Manabe and Wetherald in 1967, the change in temperature produced by a 'CO_2 doubling' during each time step is too small to measure in the normal diurnal and seasonal changes in surface temperature. The warming signal created by the 1967 model cannot accumulate in the real atmosphere.

Phase shifts, such as those described by Fourier, are observed in the diurnal and seasonal temperature cycles for both ocean and land temperatures. However, before considering these phase shifts in more detail, a brief review of time dependent energy transfer processes will be provided. Additional information is provided by Clark and Rörsch (2023).

2. Climate Energy Transfer

The earth is an isolated planet that is heated by the absorption of short wave (SW) electromagnetic radiation from the sun and cooled by the emission of longwave IR (LWIR) radiation back to space. The earth's climate has been sufficiently stable over several billion years for life to evolve into its present forms. This requires an approximate planetary energy balance between the absorbed solar flux and the outgoing LWIR radiation (OLR) returned to space so that the surface temperature over most of the planet remains within the relatively narrow range needed to sustain life. Unfortunately, this has led to the misconception that there is an exact energy balance between the absorbed solar flux and the OLR that controls the surface temperature.

The earth is also a rotating water planet with an atmosphere that has an IR radiation field. Approximately 71% of the surface area is ocean. At the surface, the downward LWIR flux from the lower troposphere interacts with the upward LWIR flux from the surface to establish an exchange energy. This limits the net cooling LWIR flux (upward minus downward LWIR flux) to the emission into the atmospheric LWIR transmission window, mainly in the 800 to 1200 cm^{-1} spectral range. Within the main spectral regions of the atmospheric IR absorption and emission bands, when the surface and surface air temperatures are similar, photons are exchanged without any significant transfer of heat. In order to dissipate the absorbed solar heat, the surface must warm up so that the excess heat is removed by moist convection (evapotranspiration). This requires a thermal and/or humidity gradient at the surface-air interface. The requirement for climate stability is set by the Second Law of Thermodynamics, not the First. There is no 'magic thermostat' at the top of the atmosphere (TOA) that controls the surface temperature. The surface gradients adjust as the temperatures change and this maintains the overall energy balance.

Convection is also a mass transport process. It is coupled to both the gravitational field and the rotation (angular momentum) of the earth. As the warm air rises through the troposphere, it cools as it expands and internal energy is converted to gravitational potential energy. For dry air, the lapse rate, or change in temperature with altitude, is -9.8 °C km^{-1}. As moist air rises above the saturation level, water condenses to form clouds with the release of latent heat. This reduces the

lapse rate. The US standard atmosphere uses an average lapse rate of -6.5 °C km^{-1}. The coupling of the convection to the rotation leads to the formation of the Hadley, Ferrel and polar cell convective structure, the trade winds, the mid latitude cyclones/anticyclones and the ocean gyre circulation. In addition, the troposphere functions as an open cycle heat engine that transports part of the absorbed solar heat from the surface to the middle and upper troposphere by moist convection. From here it is radiated back to space, mainly by LWIR emission from the water bands. The upward and downward LWIR flux terms are decoupled by molecular line broadening effects, Clark and Rörsch (2023). When the atmospheric concentration of a greenhouse gas such as CO_2 is increased, there is a slight decrease in the LWIR flux at TOA produced by absorption in the atmopshere below. A small amount of additional heat is released into the tropopshere. This is dissipated by wideband LWIR emission to space and does not produce a measurable change in surface temperature. A change in flux at TOA is called a radiative forcing by the IPCC, Ramaswamy et al, (2019). Such a forcing by greenhouse gases does not change the energy balance of the earth, nor does it produce a measurable change in surface temperature.

A change in surface temperature is produced by a change in the heat content or enthalpy of the surface reservoir or thin layer of ocean or land at the surface-air interface. There are four main, time dependent, interactive flux terms that are coupled to this reservoir. These are the absorbed solar flux, the net LWIR emission, the moist convection (evapotranspiration) and the subsurface transport (precipitation and freeze/thaw effects are not included here). The net LWIR flux increases with decreasing humidity and decreases with increasing cloud cover. The convection depends on the temperature difference between the surface and the surface air layer. The energy transfer processes are different at the land-air and ocean-air interfaces and have to be considered separately. In addition, the ocean surface temperatures are coupled to the land surface temperatures by weather systems that form over the oceans and move overland.

Over the oceans, the surface is almost transparent to the solar flux. Approximately half of the flux is absorbed within the first meter layer and 90% is absorbed within the first 10 m layer, Clark (2013a, 2013b). The diurnal temperature rise at the surface is quite small, typically 2 °C or less. The dominant cooling term is the wind driven evaporation or latent heat flux. The LWIR flux is absorbed within the first 100 micron layer, Hale and Querry (1973). Here it is fully coupled to the wind driven evaporation or latent heat flux. The sensible heat flux term is usually small, less than 10 W m^{-2}. The cooling terms are fully coupled at the surface and should not be separated and analyzed independently of each other. The cooler water produced at the surface then sinks and is replaced by warmer water from below. This is a Rayleigh-Benard type of convective flow with columns of warmer and cooler water moving in opposite directions. It is not a simple diffusion process. The convective flow and therefore the evaporative cooling continue over the full 24 hour diurnal cycle. As the cooler water sinks, it carries the surface momentum to lower depths. This drives the ocean currents that form the ocean gyre circulation. Outside of the tropics there is a seasonal time delay or phase shift between the peak solar flux at solstice and the surface temperature response that may reach 6 to 8 weeks. In addition, there is no requirement for an exact flux balance between the solar heating and the surface cooling terms. There are natural variations or quasi-periodic oscillations in ocean surface temperatures that may extend to depths of 100 m or more. This also means that there is no exact planetary flux balance at TOA between the absorbed solar flux and the OLR.

Over land, all of the flux terms are absorbed by a thin surface layer. The surface temperature increases in the morning after sunrise as the solar flux is absorbed. This establishes a thermal gradient with both the cooler air above and the subsurface ground layers below. The surface-air gradient drives the evapotranspiration and the subsurface gradient conducts heat below the surface during the first part of the day. Later in the day, as the surface cools, the subsurface gradient reverses and the stored heat is returned to the surface. As the land and air temperatures equalize in the evening, the convection stops and the surface cools more slowly by net LWIR emission. This convection transition temperature is reset each day by the local weather system passing through. Almost all of the absorbed solar heat is dissipated within the same diurnal cycle.

The surface or skin temperature is the temperature at the surface-air interface. The weather station temperature or meteorological surface air temperature (MSAT) is the temperature measured by a thermometer installed in a ventilated enclosure located for convenience near eye level, 1.5 to 2 m above the ground, Oke (2016). Historically in the US, the daily minimum and maximum MSATs were recorded using Six's thermometer mounted in a white painted wooden enclosure (Stevenson screen or cotton region shelter). Temeratures are now recorded electronically using a smaller 'beehive' enclosure. The minimum and maximum MSAT are produced by different physical processes. The minimum MSAT is usually a measure of the surface air temperature of the local weather system passing through. The change in temperature or ΔT from minimum to maximum is determined by the mixing of the warm air rising from the solar heated surface with the cooler air at the level of the MSAT thermometer. The minimum and maximum readings are often averaged to give an 'average daily temperature'. This has little physical meaning.

The energy transfer processes associated with the surface energy transfer and the tropospheric heat engine are shown schematically in Fig. 1.

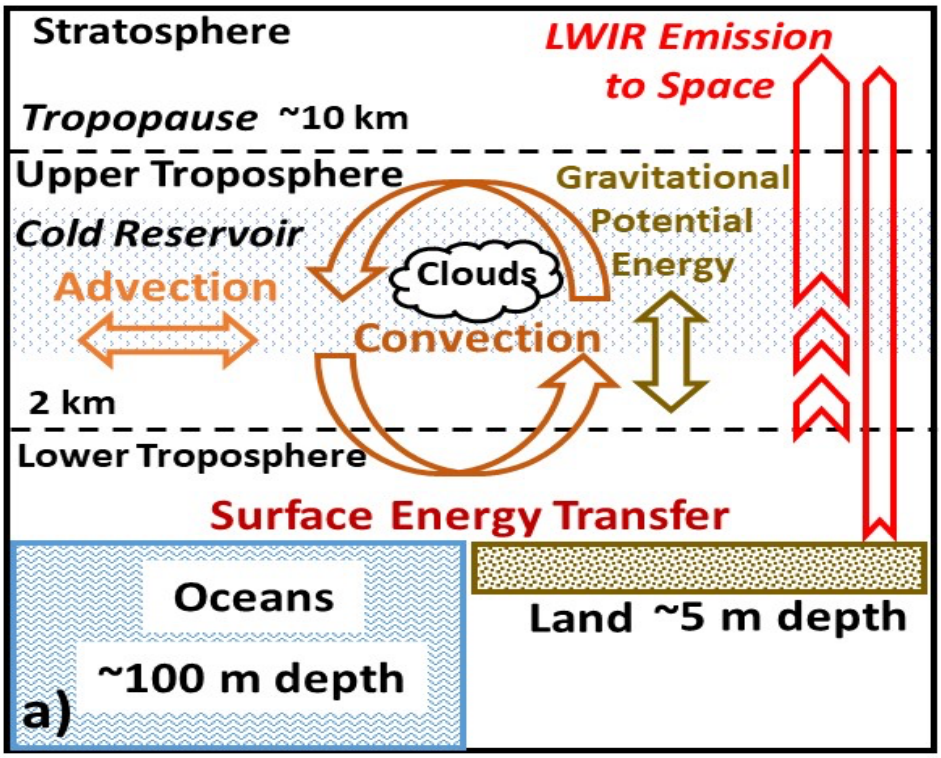

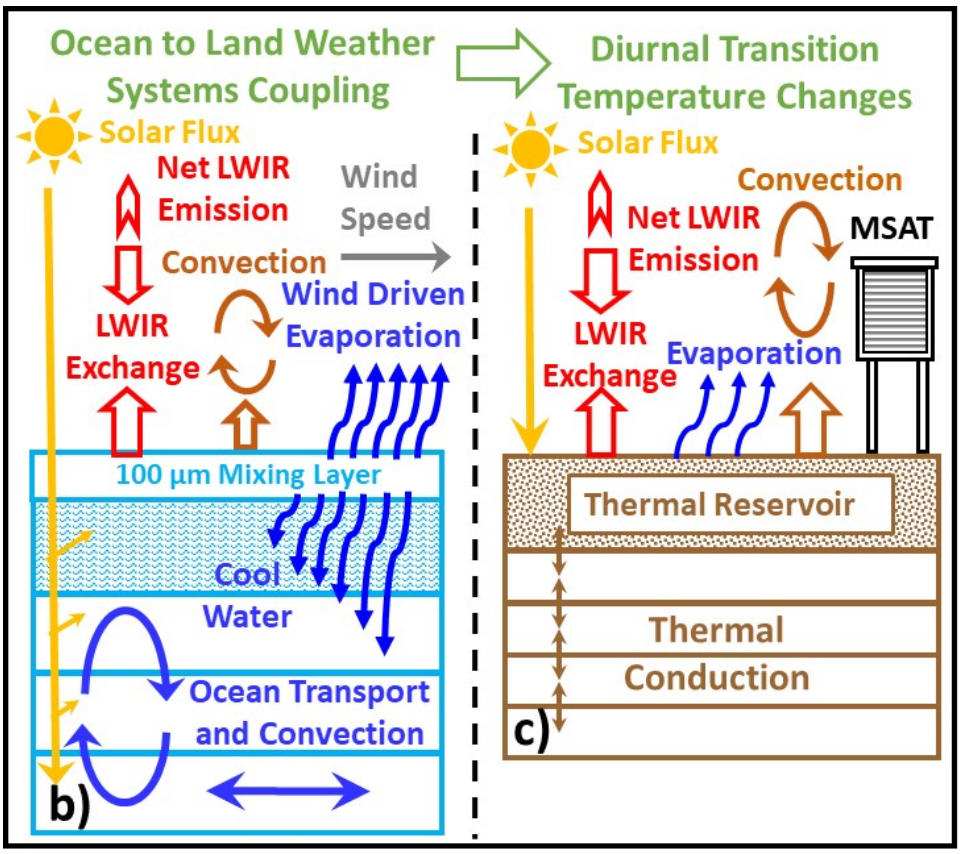

Figure 1: Basic climate energy transfer processes for the earth, a) atmospheric energy transfer showing the tropospheric heat engine, b) ocean energy transfer and c) land energy transfer (schematic).

The focus of this article is on the null hypothesis that changes in the atmosperhic concentration of greenhouse gases do not cause climate change. Short term climate change is related to quasi-periodic ocean oscillations with periods in the 1 to 7 and 10 to 70 year range. Longer term climate changes in the 100 to 1000 year time frame are related to variations in the solar activity as measured by sunspot cycles and other solar pameters. Ice age cycles with periods near 100,0000 years are caused by changes to the earth's orbital and axial rotation known as Milankovitch cycles. Over longer geological time scales, climate change is produced by plate tectonics that alter the continental boundaries that determine ocean circulation, Clark and Rörsch (2023). Natural climate drivers were recently considered by Ollila (2023). The detailed energy transfer processes related to climate change are both subtle and complex. The first step is to abandon the pseudoscience of radiative forcings, feedbacks and climate sensitivity and consider instead the time dependence of the climate energy tranfer processes that determine the surface temperature, including the phase shifts that were described by Fourier almost 200 years ago.

3. The Diurnal Ocean Phase Shift

When the solar flux warms the ocean during the day, there is a time delay or phase shift between the peak solar flux at local noon and the surface temperature response. The magnitude of both the temperature increase and the time delay are dependent on the wind speed.

Fig. 2 shows selected TRITON buoy data for location 156° E, 0° lat. (equator) in the Pacific warm pool, TRITON (2021). Hourly average data are shown for July 1 to 15, 2010. Fig. 2a shows the

air temperature and the ocean temperatures at 1.5 and 25 m depth (SST 1.5 and SST 25). Fig. 2b shows the wind speed and the solar flux. Over the period shown, the average air temperature was 301.2 K (28.2 °C), the averge SST was 301.8 K (28.8 °C) for SST 1.5 and 301.6 K (28.6 °C) for SST 25. Both the air and the SST 1.5 temperatures exhibit a diurnal variation. The maximum daily excursion was 1.5 K for the air temperature and 1 K for SST 1.5. The SST 1.5 data show a strong dependence on the wind speed. The maximum increase in daily temperature of 1 K on day 10 occurred with the wind speed near 1 m s^{-1}. The minimum increase in temperature of 0.1 K occurred on day 14 when the wind speed was in the 6 to 7 m s^{-1} range. These maxima and minima are indicated by the arrows in Fig. 2. There was a gradual drift in SST 25, but there was no significant diurnal variation at these depths.

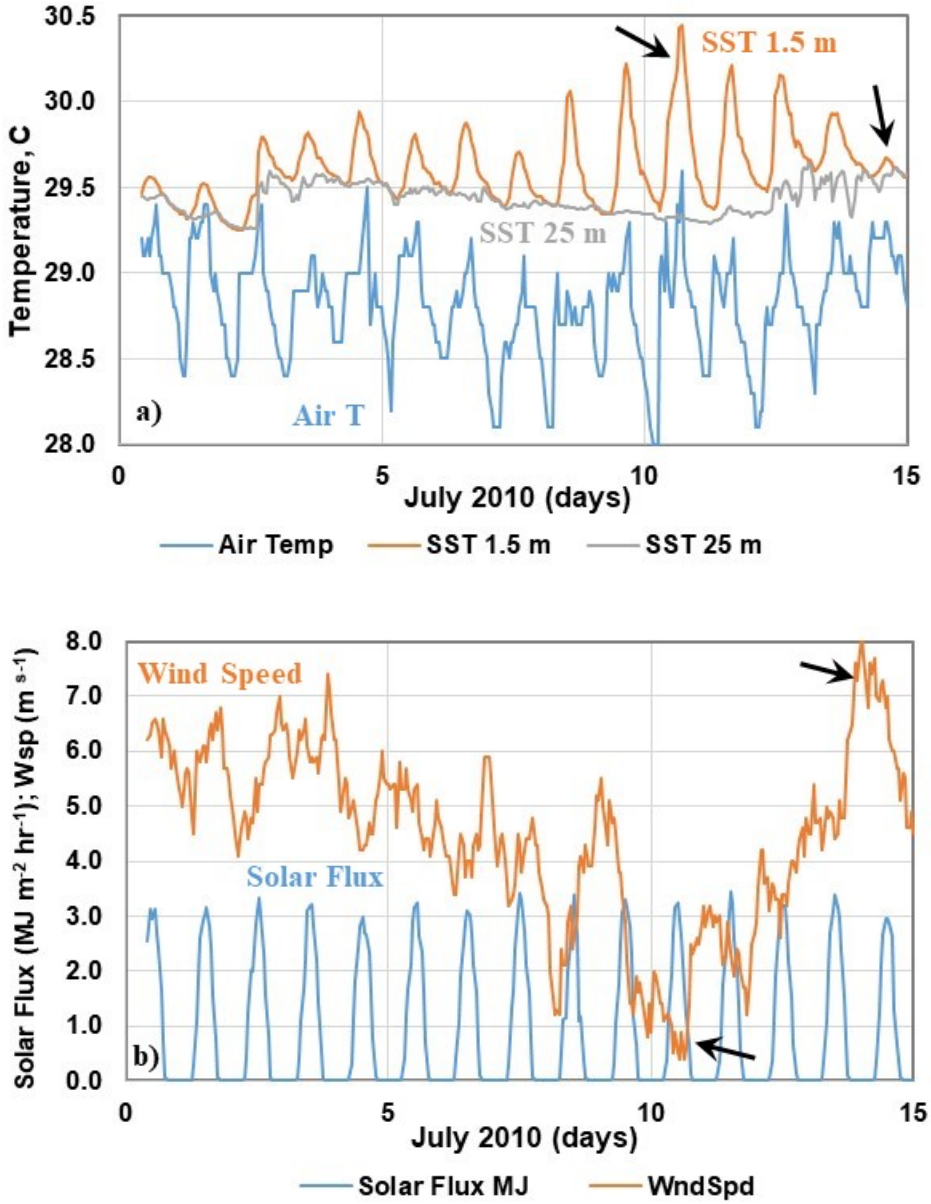

Figure 2: July 2010 TRITON buoy hourly data, 156° E, 0° lat., a) air and ocean temperatures (1.5 and 25 m), b) wind speed and solar flux.

The magnitude of the phase shift is also dependent on the wind speed. This is shown in Fig. 3 for days 10 to 15. The approximate phase shift in hours and the total daily solar flux in MJ m^{-2} day^{-1} are shown for each of the 5 days. The phase shift decreases as the wind speed increases. This increases the surface evaporation and there is more downward convection of cooler water from the surface. The sensitivity of the latent heat flux to the wind speed is approximately 15 W m^{-2}/m s^{-1}, Clark and Rörsch (2023). In addition, the 1 to 2 MJ m^{-2}.day^{-1} variations in the total daily solar flux have no observable effect on the SST 1.5 diurnal temperature changes. The increase in downward LWIR flux to the surface produced by an increase of 140 ppm in the atmospheric CO_2 concentration is approximately 2 W m^{-2} or 0.17 MJ m^{-2}.day^{-1}. This can have no measurable effect on ocean temperatures. It is simply absorbed within the first 100 micron ocean layer and dissipated as an insignificant part of the total surface cooling flux. The absorbed solar flux is decoupled from the wind speed driven latent heat flux. There is no 'equilibrium average flux balance' at the ocean surface on any time scale. The amount of heat stored in the ocean thermal reservoir depends on the accumulated net flux balance, including ocean transport effects. There can be no 'climate sensitivity' to CO_2.

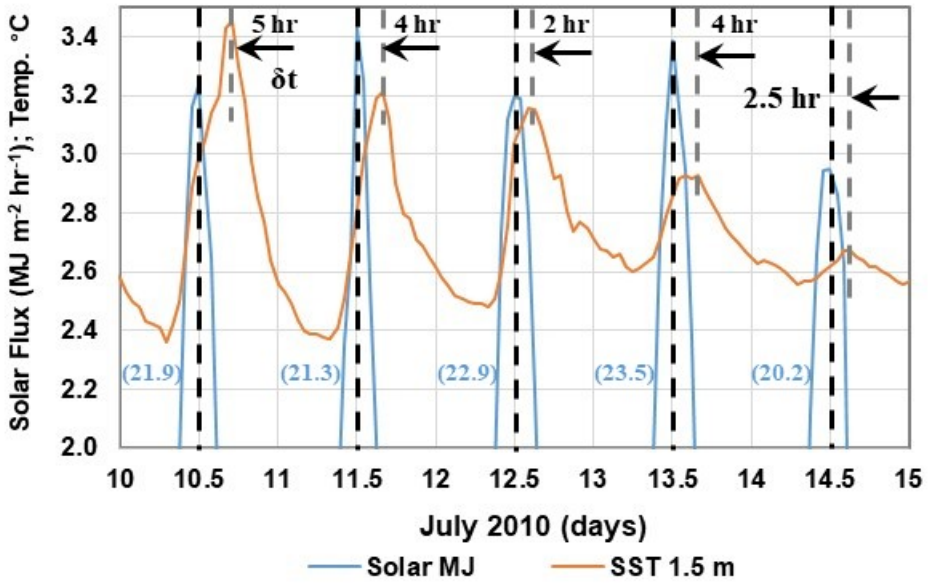

Figure 3: Phase shift between the 1.5 m ocean temperature and the solar flux, July 10 to 15, 2010. The values for the total daily solar flux (MJ m^{-2} day^{-1}) are also shown in parenthesis.

4. The Seasonal Ocean Phase Shift

Fig. 4 shows the monthly ocean temperatures for 2018 at selected depths from 2.5 to 200 m for a 5° x 1° (latitude x longitude) strip at 10° intervals from 60° N to the equator, 0° N along the 20° longitude transect in the N. Atlantic Ocean. This extends from south of Iceland to the equator off the coast of Africa as shown on the location map. The data were downloaded from the Argo Marine Atlas, Argo (2021). For latitudes from 20° to 60° N, the data show a winter surface temperature minimum in March or April. Summer solar heating then produces a stable stratified thermal layer structure with a surface temperature peak in August or September. The peak temperatures increase from 10 °C at 60° N to 25 °C at 20° N. There is a time delay or phase shift of approximately 8 weeks after summer solstice. The phase shift increases and temperature rise decreases at lower depths. The subsurface thermal layer structure then collapses as the wind driven evaporative cooling in winter exceeds the solar heating. The heat stored and released during the

course of a year may easily reach 1000 MJ m^{-2}. This is a major factor in stabilizing the earth's climate. At low latitudes, 0° and 10° N, there is no obvious summer temperature peak. These locations are influenced by the S. Atlantic Equatorial Current. The cooler water from the Benguela Current that flows northwards along the west coast of Africa, changes direction and flows westwards towards S. America. For 0° N, the surface temperature increases from approximately 27 to 29 °C for the first five months of the year. It then decreases to approximately 24 °C over the next three months and gradually warms up during the rest of the year. The April peak is produced by the summer solar heating in the S. Hemisphere.

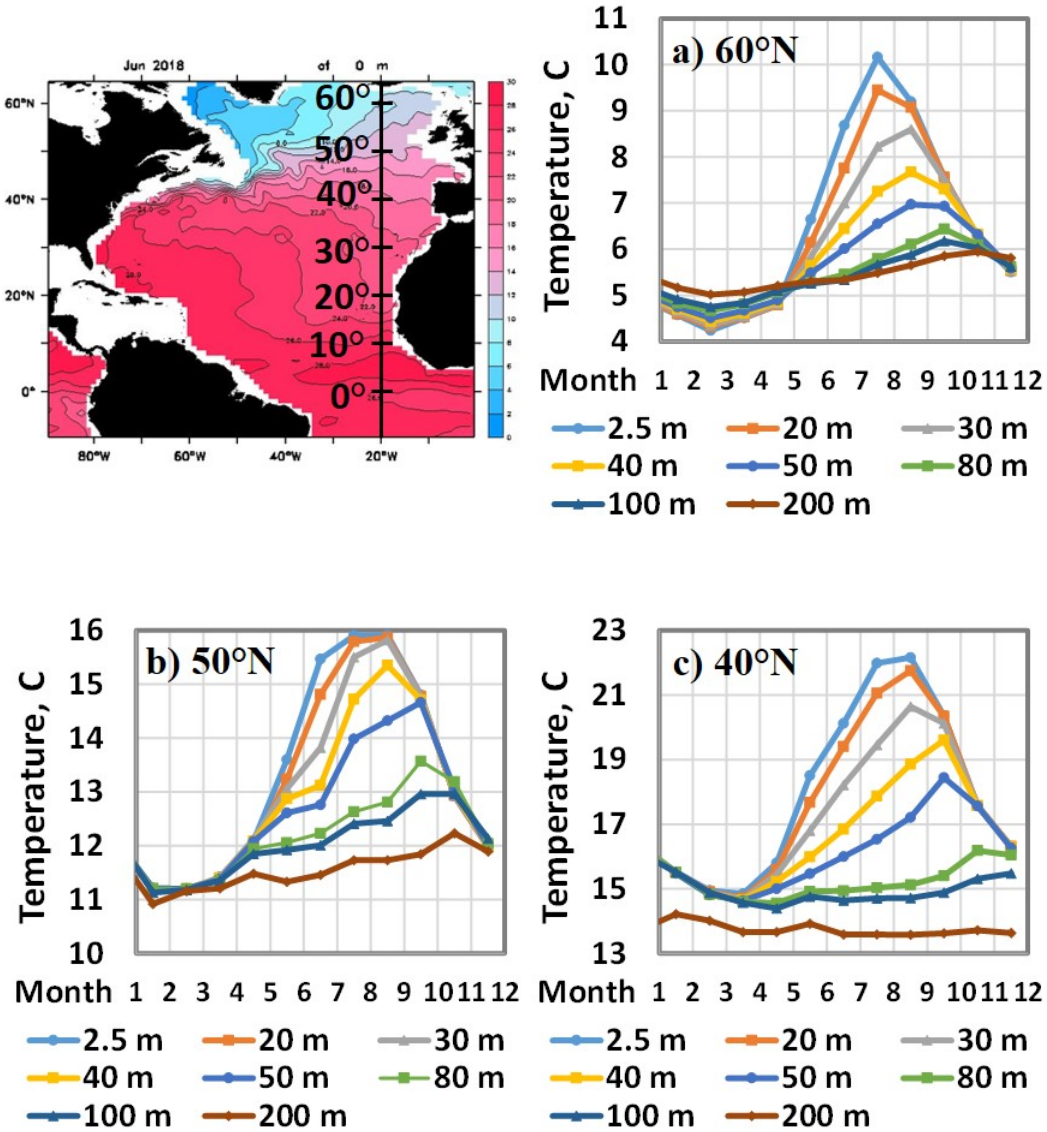

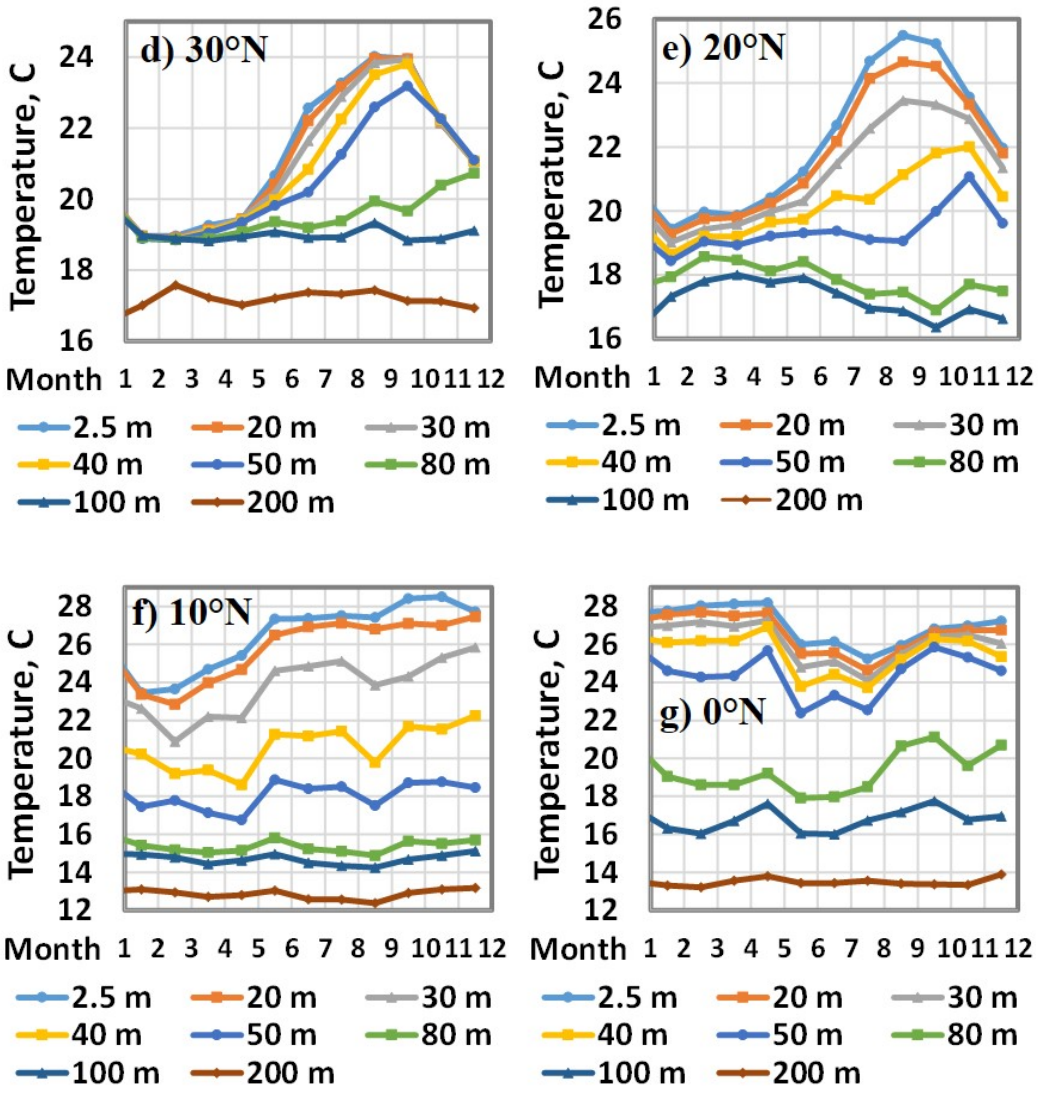

Figure 4: Monthly Argo float data for 2018 for selected depths from 2.5 to 200 m at 10° intervals from 60° N to the equator along the 20° W longitude transect. The locations are indicated on the map, inset.

5. The Diurnal Phase Shift Over Land

Historically in many countries, the maximum and minimum MSATs were recorded using Six's thermometer. The diurnal phase shift was only recorded during specialized measurement programs. It was recorded in 1953 as part of the Great Plains Turbulence Field Program conducted in O'Neill, Nebraska, (Letteau and Davidson 1957; Clark and Rörsch 2023). Subsurface temperature data and the 2 m air temperature recorded for August 13-14, 1953, are shown in Fig. 5. The phase shift for the surface (0.5 cm) temperature is indicated. The measurement site latitude and longitude are 42° 26' N and 98° 32' W. Local solar noon occurs approximately 30 minutes after Central Standard Time (CST) noon. The minimum surface temperature of 18.7 °C was recorded at 06:30 and the maximum surface temperature of 40.9 °C was recorded at 14:30. At the end of the observation period at 02:30 on August 14, the temperature was 20.6 °C. The temperature may be expected to continue to cool until after sunrise. The diurnal temperature rise decreased with increasing depth and the phase shift increased with depth. The diurnal temperature variations were not detectable at 80 cm depth. The surface and air temperatures equalized near 6.30 pm. The convection transition temperaure was near 31 °C.

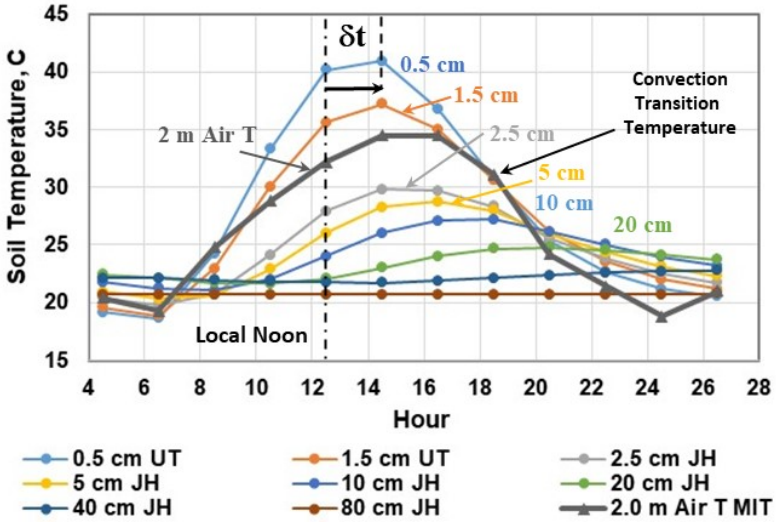

Figure 5: Subsurface temperature data and the 2 m air temperature recorded at O'Neill, Neb. on August 13-14, 1953.

The parameters recorded during this test period also included humidity and solar, total and net flux data. The absolute humidity (mb) and the relative humidity (RH %) are shown in Fig. 6. As the air temperature increased during the first part of the day after sunrise, the absolute humidity increased from 14 to 20 mb. This was caused by increased evaporation from the solar heated surface. However, the relative humidity decreased from 70 to 30%, because the saturated water vapor pressure used to determine the relative humidity increased with the air temperature. The assumption of a fixed RH used in the climate models is incorrect near the surface, Manabe and Wetherald (1967). This also invalidates the water vapor feedback used equilibrium climate models to amplify the initial temperature increase produced by an increase in CO_2 concentration, IPCC AR6 (2021). The O'Neill field data would have been available to Manabe and Wetherald before 1967.

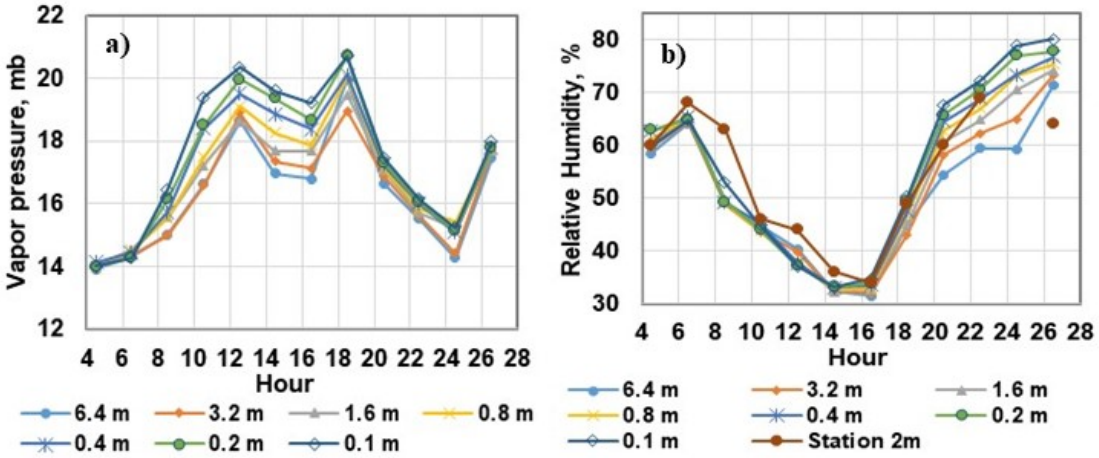

Figure 6: a) Humidity (mb) and b) relative humidity (%) at seven monitoring locations, 0.1 to 6.4 m above the surface. The weather station RH measurement is also included in b). Recorded at O'Neill, Neb. on August 13-14, 1953.

The recorded flux data is summarized in Fig. 7. The peak solar flux was 957 W m^{-2}. At night, the measured net flux is the difference between the upward LWIR flux emitted by the surface and the downward LWIR flux emitted by the lower troposphere to the surface. The average value was -59 W m^{-2}. A negative flux indicates a surface cooling. During the day, the net flux also includes the net solar flux (downward minus reflected solar flux). The total flux includes both the downward solar flux and the downward LWIR flux. There was insufficient data for a more detailed analysis.

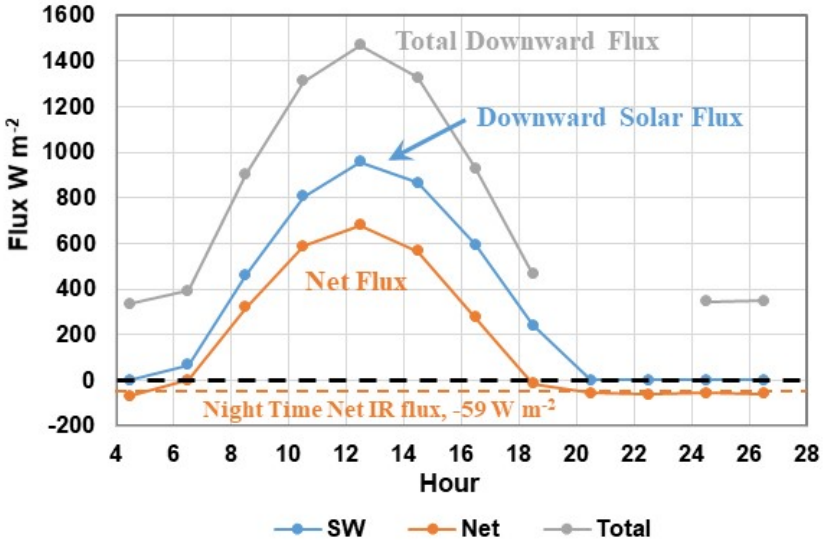

Figure 7: Total, solar and net flux data recorded at O'Neill, Neb. on August 13-14, 1953.

6. The Seasonal Phase Shift Over Land

In addition to the diurnal phase shift, there is also a seasonal phase shift. The peak temperatures occur after the summer solstice. This may be investigated by using the 1981 to 2010 30 year daily climate averages for the O'Neill, Neb. weather station #256290, WRCC, (2021). The maximum and minimum daily temperatures, the 1σ standard deviations and the ΔT (T_{max} - T_{min}) values are shown in Fig. 8. There is a phase shift of approximately 30 days between the peak solar flux at summer solstice, day 172 and the peak seasonal temperature response. In addition, the ΔT values remain within the approximate range 13.4 ±2 °C for the entire year while the temperature variation is ±10 °C. The change in temperature from one day to the next, ΔT_n, for the maximum and minimum temperatures are shown in Fig. 9. The day to day temperature changes are small, below 0.4 °C. The phase shift is indicated by the zero crossing point after the summer solstice. There are three features in Fig. 8 that require further consideration. First, the 1σ standard deviations are quite large. Second, the variation in ΔT is smaller than the changes in the max and min temperatures. Third, the seasonal phase shift is not produced locally.

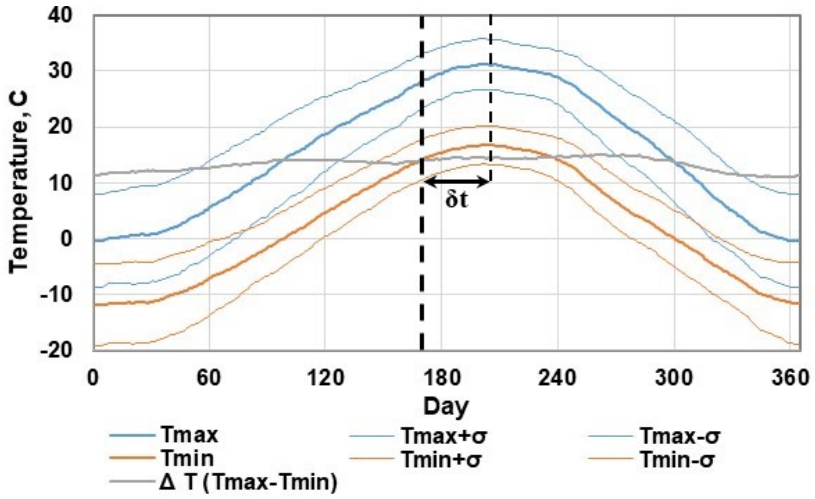

Figure 8: 1981-2010 daily climate averages for O'Neill, Neb., station #256290. The 1σ standard deviations and the ΔT (T_{max} -T_{min}) are also shown. The seasonal phase shift, δt is indicated.

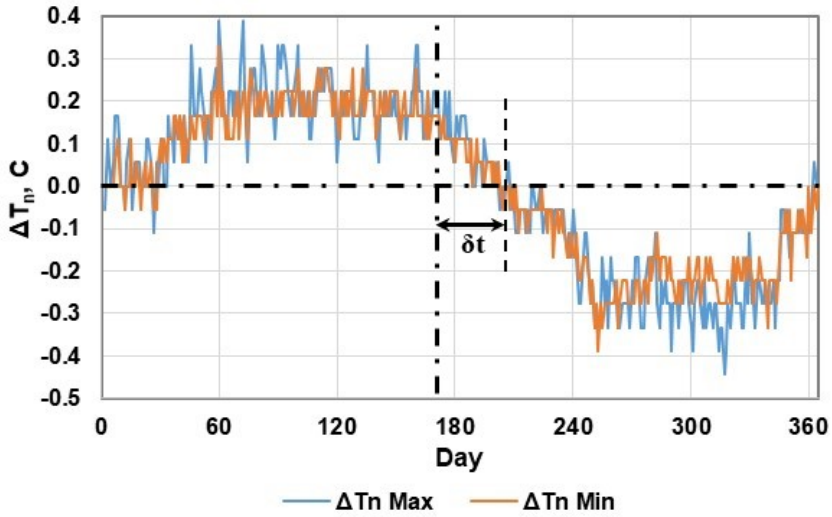

Figure 9: The change in temperature from one day to the next, ΔT_n for the maximum and minimum temperatures shown in Fig. 8. The seasonal phase shift here is the zero-crossing point after the summer solstice. The time delay is approximately 30 days.

The 1σ standard deviation range in the daily average temperatures is from ±3.4 to ±8.7 °C. The larger values occur at the beginning and end of the year when the temperatures are lower. Convective cooling of the surface occurs during the day when the solar heated surface is warmer than the surface air temperature. Each evening there is a convective transition temperature at which the surface and surface air temperatures approximately equalize and the dominant cooling term becomes the net LWIR flux emitted into the LWIR transmission window. This transition temperature is reset each day by the local weather system passing through. The variation in transition temperature is similar to the variation in the minimum temperatures. The measured maximum and minimum temperatures and ΔT values from the 1953 O'Neill observation site weather station data are plotted in Fig. 10 with the climate data from Fig. 8 over the same time period. The differences from the climate means are plotted in Fig. 11. The maximum difference is +8.8 °C for Sept 8. The day to day temperature variations related to the convection transition temperature are sufficiently

large that any change in surface temperautre produced by an increase in the downward LWIR flux to the surface related to an increase in the CO_2 concentration are too small to measure, Clark and Rörsch (2023).

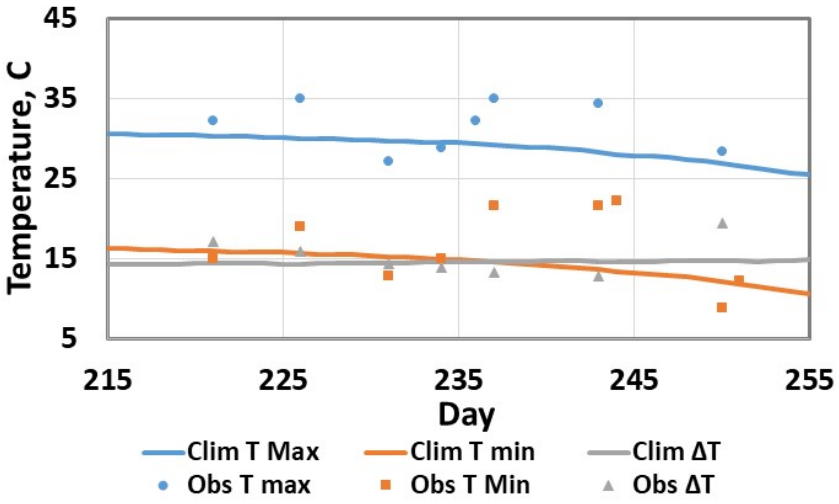

Figure 10: The maximum and minimum air temperatures and ΔT values from the O'Neill Test Site weather station data, plotted with the 1981-2010 30-year climate average data for O'Neill.

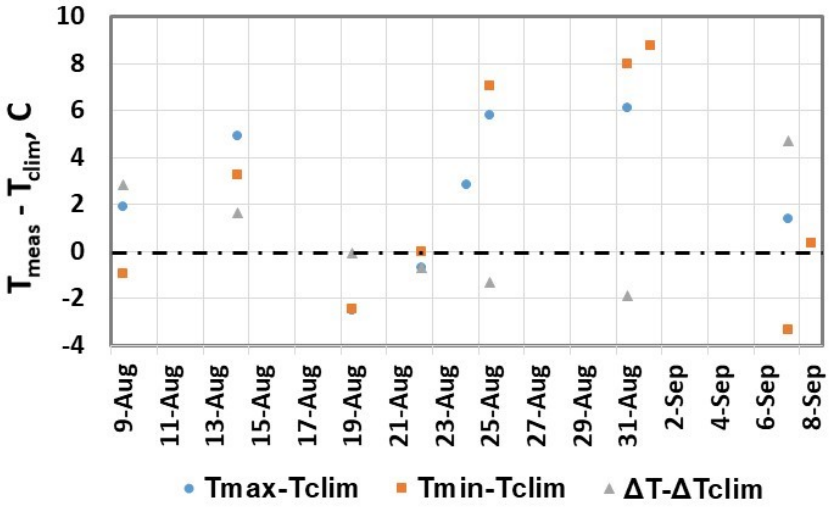

Figure 11: Deviations of the measured temperatures and delta temperatures from the climate averages shown in Figure 8.

The smaller variation in ΔT compared to the min and max temperatures shows that there is a control mechanism that regulates the daily temperature increase. The moist convection (evapotranspiration) or sensible and latent heat fluxes increase with the solar flux and the rate of surface cooling increases. The latent heat flux also depends on the available surface moisture. This is discussed in more detail by Clark and Rörsch (2023).

Over land, almost all of the absorbed solar flux is dissipated within the same diurnal cycle. The heat capacity of the surface layer is too small to produce any large seasonal phase shifts. These are caused by changes in the convective transition temperature related to the weather systems passing through. In many regions of the world, these weather systems are formed over the ocean and the bulk air temperature is influenced by the ocean temperature along the path of the weather system. The source of the seasonal phase shift is the ocean temperature response to the solar flux. There may also be longer term temperature fluctuations related to ocean oscillations.

7. The Coupling of the Ocean and Land Surface Temperatures

The ocean to land coupling of the surface temperatures may be investigated by comparing Pacific Ocean surface temperatures off the coast of California to land surface temperatures measured at the Ameriflux 'Grasslands' monitoring site near Irvine, CA and the daily 1981-2010 climate record from the nearby Santa Ana weather station. Fig. 12 shows the 2.5 m depth ocean temperatures for 2017 derived from Argo float data. The data are for rectangular areas centered at 35° and 45° N, 127.5° W. The angular block size is 2° latitude and 5° longitude. The size was selected to provide an average of at least 10 Argo buoy readings per month near the coast along the path of the prevailing weather systems approaching California from the Gulf of Alaska. The Argo data consists of monthly averages. These were fit to 5th order polynomials that were used to generate the daily trends. In addition, the 30 year average MSAT minimum data for Santa Ana, WRCC, (2021) and the MSAT minimum data for the Grasslands site (Clark and Rörsch 2023; Clark, 2013a; 2013b) are also shown. The seasonal phase shift and the temperature range are consistent with ocean temperatures near 45° N. The temperature spikes in the Grasslands data are produced by the transition from onshore ocean air flow to offshore flow. As the air flows from the inland desert plateau to the ocean it descends by approximately 1 km in altitude and is warmed by air compression.

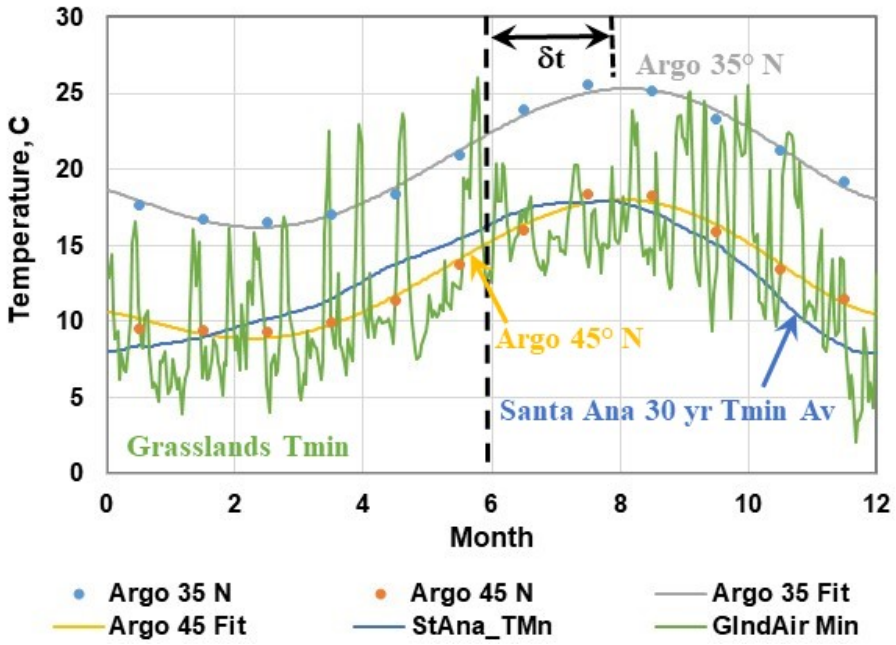

Figure 12: Comparison of Argo 2.5 m ocean surface temperatures at 35° and 45° N with the 30 year 1981-2010 daily minimum MSAT from Santa Ana and the Grasslands 2008 minimum MSAT data.

The seasonal phase shifts observed for Santa Ana are not limited to coastal weather stations. They are observed in weather stations across the continental US and in many other regions of the world. Fig. 13a and 13b shows the 1981-2010 30 year daily T_{min} and T_{max} climate data for eight S. California weather stations, WRCC (2021). The locations are indicated on the map. Los Angeles (LA) and Los Angeles Airport (LAX) are located near or at the coast. The maximum temperatures here are lower because of the influence of the ocean marine layer. The nighttime cooling is also less. Redlands (Rdl), Riverside (Rvsd) and San Bernardino (SnBno) are located approximately 80 km (50 miles) inland, Indio (Ino) and Mecca (Mca) are approximately 150 km (94 miles) inland and Blythe (Bly) is approximately 250 km (156 miles) inland near the Colorado River. The approximate phase shift is indicated. The ΔT temperature rises from min to max are shown in Fig. 13c.

These stay in a narrower range than the measured temperatures. The seasonal phase shifts are shown in Fig. 13d. These vary from approximately 60 to 30 days. The values generally decrease with increasing distance from the coast. Fig. 14 shows the 30 year daily 1981-2010 climate data, ΔT temperature rise and seasonal phase shifts for 11 US stations near 40° latitude.

In addition to the seasonal phase shift, longer term temperature changes related to ocean oscillations are also coupled to the weather station temperatures through the convection transition temperature. For California stations, the Pacific Decadal Oscillation (PDO) can be detected and for UK stations it is the Atlantic Multi-decadal Oscillation (AMO). This is discussed in more detail in Clark and Rörsch (2023).

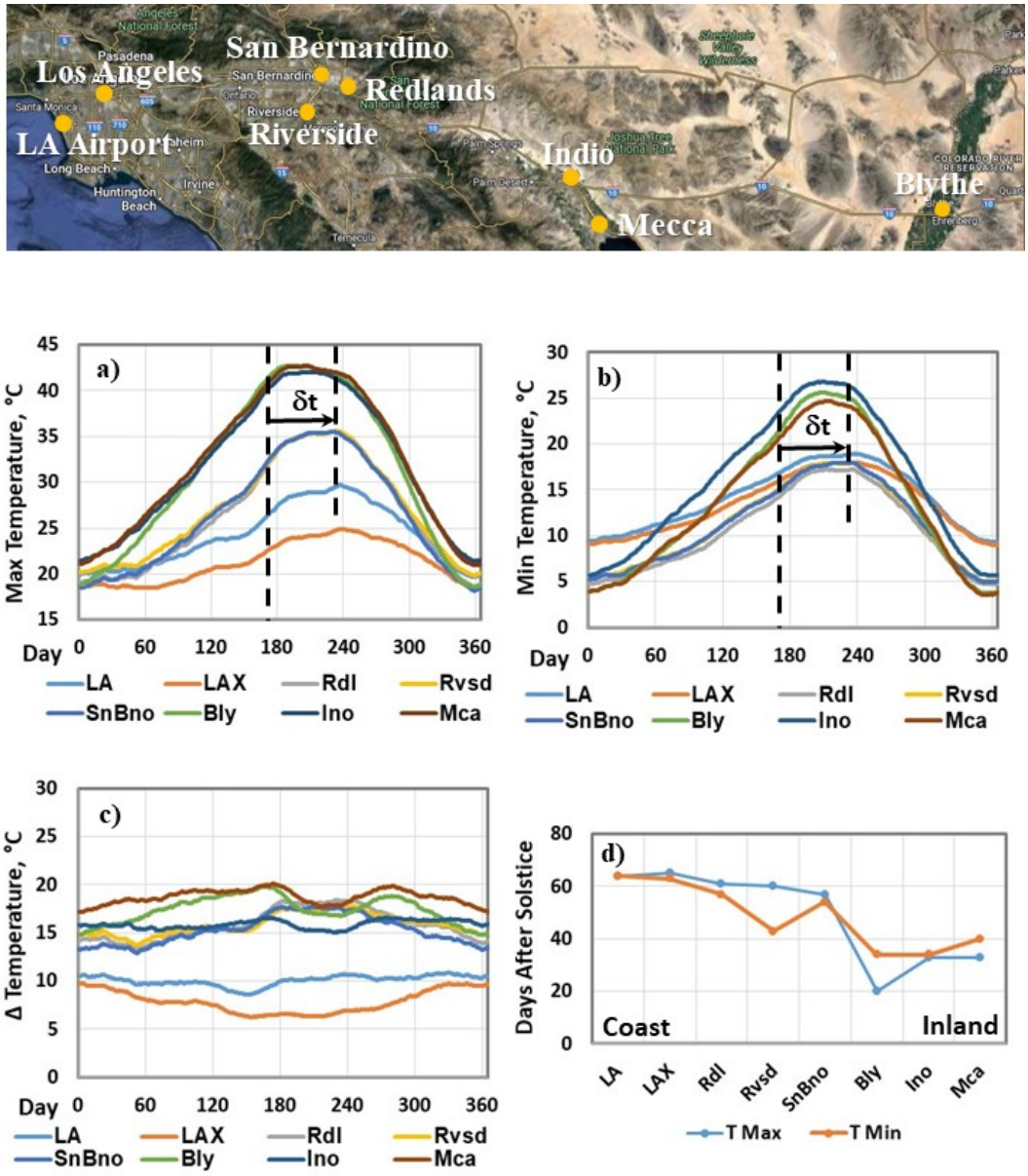

Figure 13: Daily climate averages for a) minimum, b) maximum, c) ΔT (max-min) temperatures and d) the seasonal phase shifts for eight weather stations in S. California, Los Angeles (LA), Los Angeles Airport (LAX), Redlands (Rdl), Riverside (Rvsd), San Bernardino (SnBno), Blythe (Bly), Indio (Ino) and Mecca (Mca).

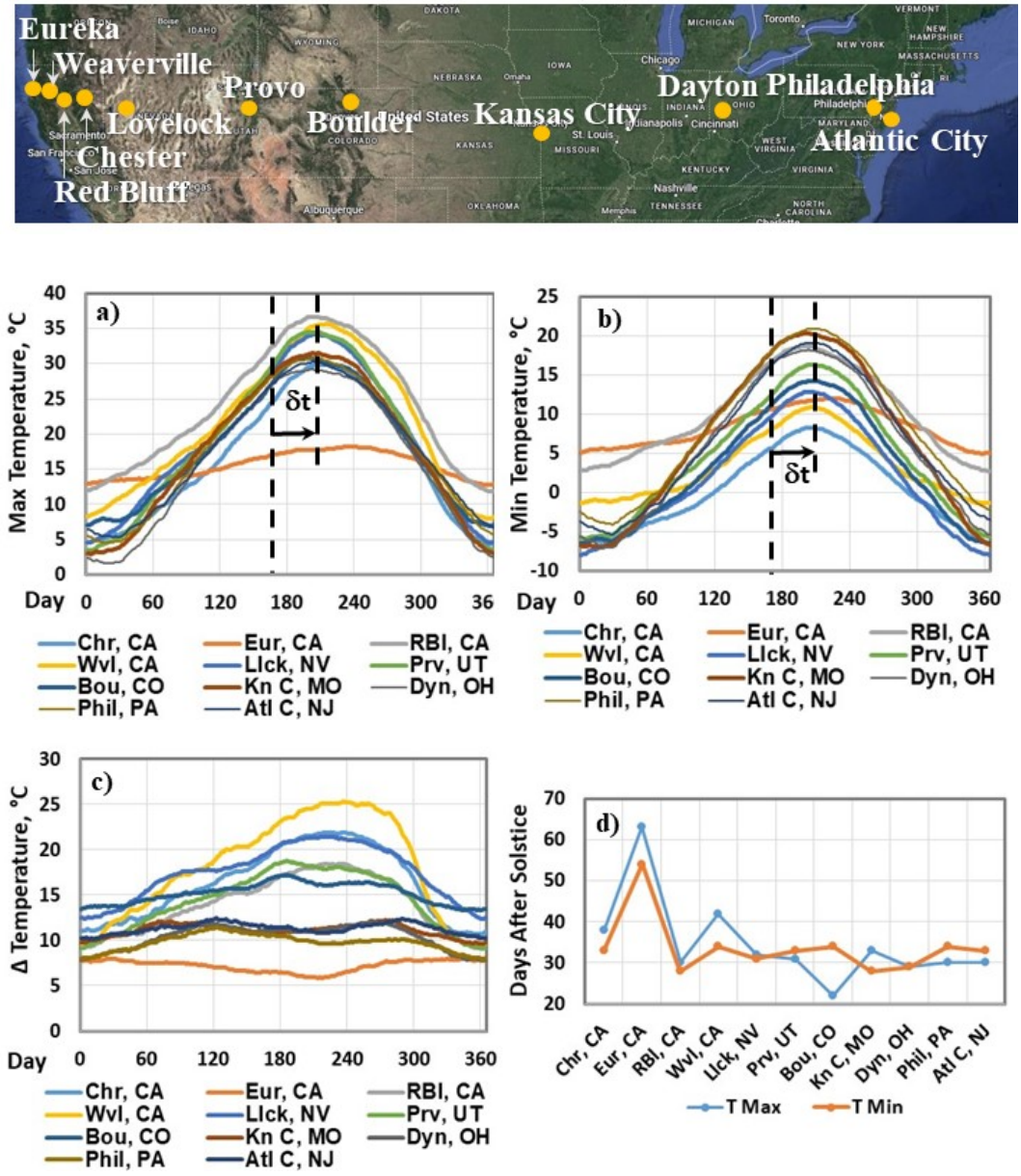

Figure 14: 30 year climate data and seasonal phase shifts for 11 weather stations near 40° latitude, Chester (Chr), CA, Eureka (Eur), CA, Red Bluff (RBl) CA, Weaverville (Wvl), CA, Lovelock (Llck), NV, Provo (Prv), UT, Boulder (Bou), CO, Kansas City (Kn C), MO, Dayton (Dyn), OH, Philadelphia (Phil), PA and Atlantic City (Atl C), NJ.

The global temperature change record is an area weighted average of the weather station data after it has been extensively processed or 'homogenized' and the mean has been subtracted. When the climate anomaly record, such as the HadCRUT4 data set is evaluated, the dominant term is found to be the Atlantic Multi-decadal Oscillation (AMO). The correlation coefficient between the two data sets is 0.8. This is illustrated in Fig. 15a (AMO, 2022; HadCRUT4, 2022; Morice et al, 2012). The AMO consists of a quasi-periodic oscillation superimposed on an underlying linear trend. A least squares fit to the data from 1900 gives a sinusoidal oscillation with an amplitude of 0.2 °C and a period of 61 years with a long term linear trend near 0.3 °C per century. The linear trend is attributed to the temperature recovery from the Maunder minimum or Little Ice Age, Akasofu (2010). Both the period and the slope may change with time. There is a 0.3 °C offset

between the AMO and the HadCRUT data after 1970. This requires further investigation of the 'homogenization' process and bias effects related to changes in the number and location of the weather stations used to generate the HadCRUT averages (Andrews, 2017a; 2017b; 2017c; D'Aleo and Watts, 2010). The influence of the AMO extends over large areas of N. America, Western Europe and parts of Africa. The weather systems that form over the oceans and move overland couple the ocean surface temperature to the weather station data through the diurnal convection transition temperature. The contributions of the other ocean oscillations to the global temperature anomaly are smaller. The IOD and the PDO are dipoles that tend to cancel and the ENSO is limited to a relatively small area of the tropical Pacific Ocean. However, small surface temperature variations in the tropical oceans have a major impact on ocean evaporation and rainfall. Fig. 15b shows a tree ring construction of the AMO from 1567 (Gray, 2004; Gray.NOAA, 2004). The modern instrument record is also indicated in green.

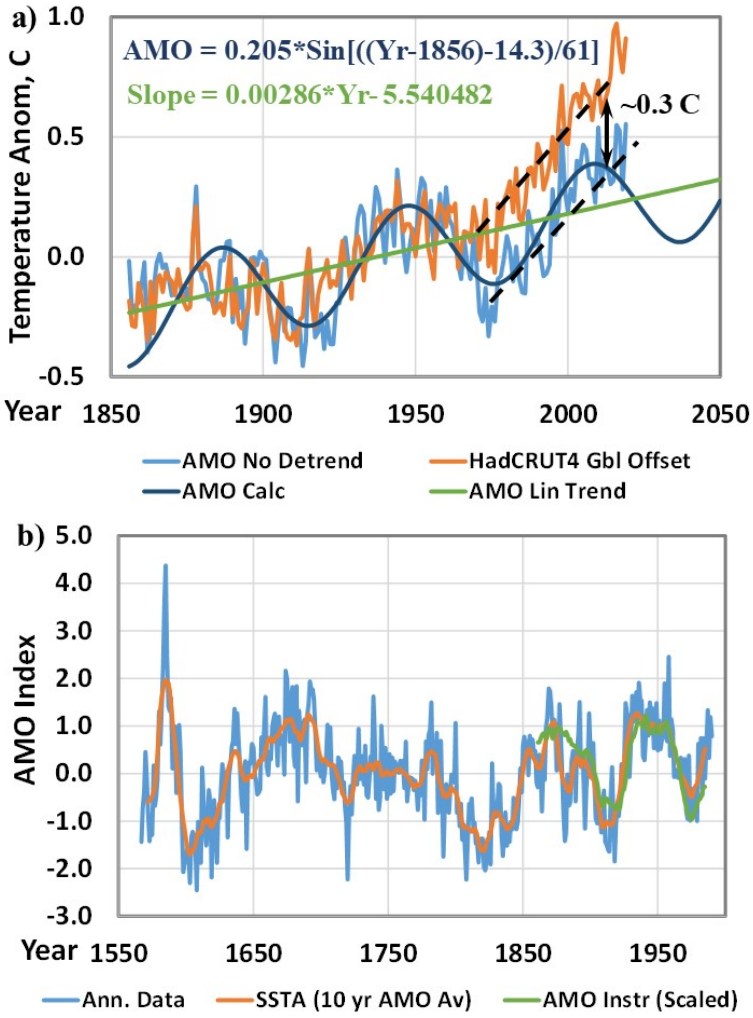

Figure 15: a) Plots of the HadCRUT4 and AMO temperature anomalies overlapped to show the similarities. Both the long term 60 year oscillation and the shorter term 'fingerprint' details can be seen in both plots. b) Tree ring reconstruction of the AMO from 1567. The modern instrument record is shown in green.

The role of the AMO in setting the surface air temperature has been misunderstood or ignored for a long time. The first person to claim a measurable warming from an increase in CO_2 concentration was Callendar (1938). The warming that he observed was from the 1910 to 1940 warming phase of the AMO not from CO_2. This was coupled to the land-based weather stations through changes to the convection transition temperature. During the 1970s there was a 'global cooling'

scare that was based on the cooling phase of the AMO from 1940 to 1970 (McFarlane, 2018; Peterson et al, 2008; Douglas, 1975; Bryson and Dittberner, 1976). In their 1981 paper Hansen et al chose to ignore the 1940 AMO peak in their analysis of the effects of CO_2 on the weather station record, Hansen et al (1981). Similarly, Jones et al conveniently overlooked the 1940 AMO peak when they started to ramp up the modern global warming scare in (Jones et al, 1986; 1988). The IPCC also ignored the AMO peak in its First Assessment Report in 1990, IPCC FAR WG1 fig. 11 SPM p. 29, IPCC FAR (1990) and it has continued to ignore it as shown in IPCC AR6 WG1 TS CS Box 1 fig. 1c p. 61, IPCC, AR6, (2021). This is illustrated in Fig. 16. The AMO, the HadCRUT4 global data and the periods of record used are shown in Fig. 16a. The AMO consists of a long period oscillation near 60 years superimposed on a linear temperature recovery from the Little Ice Age (LIA), Akasofu (2010). The temperature records used by Callendar, Douglas, Jones et al, Hansen et al and IPCC 1990 and 2021are shown in Figs. 16b through 16g. The Keeling curve showing the increase in atmospheric CO_2 concentration is also shown in Figs. 16d through 16g, Keeling (2023).

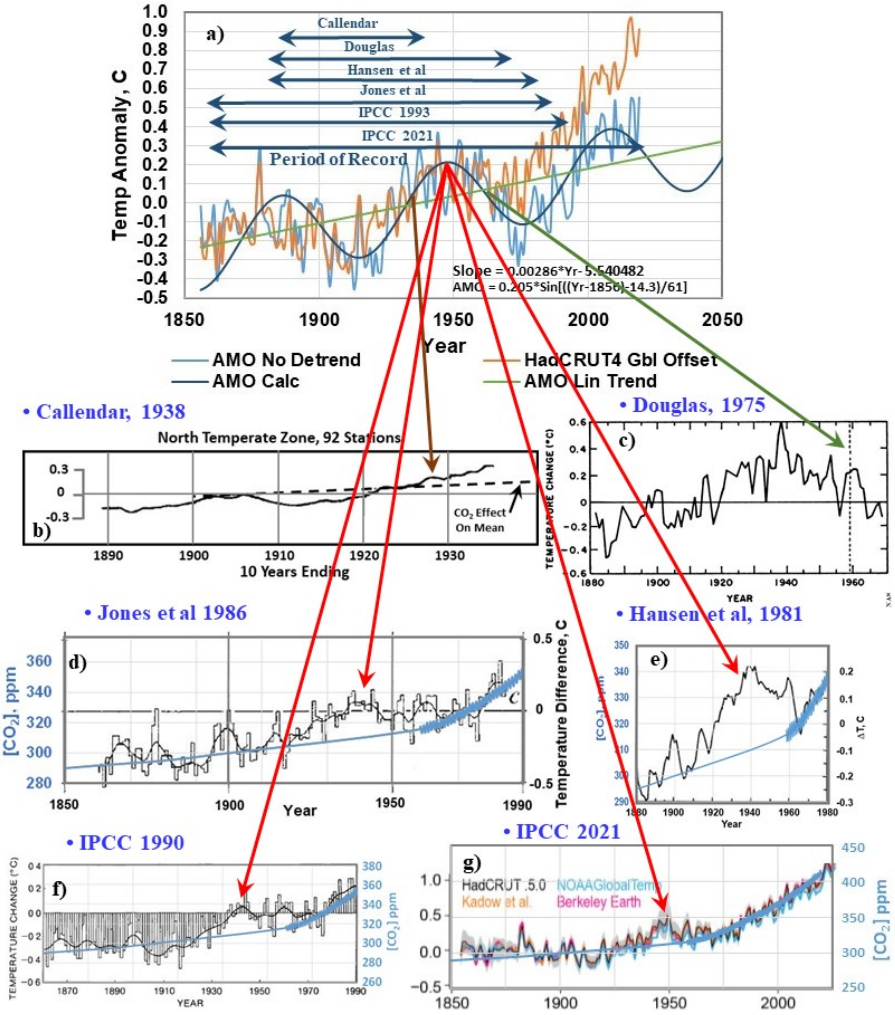

Figure 15: a) AMO anomaly and HadCRUT4 global temperature anomaly, aligned from 1860 to 1970, b) temperature anomaly for N. temperate stations from Callendar (1938), c) global cooling from Douglas (1975), d) global temperature anomaly from Jones et al (1986), e) global temperature anomaly from Hansen et al (1981), f) and g) global temperature anomaly from IPCC (1990) and IPCC (2021). The changes in CO_2 concentration (Keeling curve) are also shown in d) through g). The periods of record for the weather station data are also indicated.

8. Conclusions

The time delays or phase shifts between the peak solar flux and the surface temperature response are an important and long neglected part of the time dependent surface energy transfer processes that determine the surface temperature. The subsurface seasonal land temperature phase shift was described by Fourier in 1824 and 1827. Diurnal and seasonal phase shifts occur in both the ocean and land temperature records. Such phase shifts are clear evidence for a non-equilibrium thermal response to the solar flux. Starting with the work of Pouillet in 1836, this time dependence was neglected and replaced by an equilibrium average 'climate'. It was assumed, incorrectly, that the surface temperature could be determined using average values for just the solar and IR flux terms. Physical reality was abandoned in favor of mathematical simplicity. The scientific process of hypothesis based on available evidence was not applied. The equilibrium climate assumption became accepted as scientific dogma that provided foundation for the pseudoscience of radiaitve forcings, feedbacks and climate sensitivity still used by the IPCC today.

Over the oceans there is a diurnal phase shift where both the temperature rise and the time delay are dependent on the wind speed. This is because the dominant surface cooling term is usually the wind driven evaporation or latent heat flux. Outside of the tropics there is also a significant seasonal phase shift that may easily reach 6 to 8 weeks. There is no requirement for an exact flux balance between the absorbed solar heat and the surface cooling. Any thermal imbalance is accounted for by a change in ocean heat content or enthalpy. The penetration depth of the LWIR radaition into the surface is 100 micron or less. Here it is fully coupled to the wind driven evaporation. Any small increase in downward LWIR flux to the surface is overwhelmed by the much larger and more variable latent heat flux. Small increases in the downward LWIRflux to the surface produced by a 'greenhouse gas forcing' cannot produce a measurable incease in ocean surface temperature.

Over land, the excess absorbed solar heat is removed during the day by moist convection. Almost all of the absorbed solar flux is dissipated within the same diurnal cycle. The surface temperature is reset each day as the bulk air temperature of the local weather system changes the diurnal transition temperature. In many parts of the world, the prevailing weather systems are formed over the oceans and then move overland. This explains the observed coupling of the seasonal phase shift in the ocean surface temperature to the weather station record. On a longer timescale, the ocean oscillations may also be coupled to the weather station record.

There can be no 'CO_2 signal' in the global mean temperature record. The dominant term is the AMO. There are also contributions from urban heat island effects and changes to the number and urban/rural mix of the weather stations used in the averaging. The raw data is also adjusted for bias using homogenization techniques that generally add warming to the raw data. The 1940 AMO peak in the temperature record has been conveniently ignored.

The equilibrium assumption is still the foundation of the fraudulent climate models in use today. When the time dependent surface temperature changes related to the diurnal and seasonal cycles are analyzed in more detail, it is found that there can be no 'climate sensitivity' to CO_2. The changes in LWIR flux related to a 'radiative forcing' by greenhouse gases do not change the energy balance or the surface temperature of the earth. Nor can there be a 'water vapor feedback' that amplifies a nonexistent warming. This is a mathematical artifact created by the equilibrium assumption, the fixed RH distribution and the time step integration algorithm introduced by Manabe and Wetherald in 1967.

Guest-Editor: Stein Storlie Bergsmark; Reviewers: anonymous.

Acknowledgements

This work was performed as independent research by the author. It was not supported by any grant awards and none of the work was conducted as a part of employment duties for any employer. The views expressed are those of the author.

References

Akasofu, S.-I., 2010: *On the recovery from the Little Ice Age*, Natural Science, v. 2, no. 11, pp. 1211-1224. http://dx.doi.org/10.4236/ns.2010.211149

AMO, 2022: *Atlantic Multidecadal Oscillation*. https://www.esrl.noaa.gov/psd/data/correlation/amon.us.long.mean.data

Andrews, R., 2017a: *Adjusting Measurements to Match the Models – Part 3: Lower Troposphere Satellite Temperatures*, Energy Matters, Sept 14. http://euanmearns.com/adjusting-measurements-to-match-the-models-part-3-lower-troposphere-satellite-temperatures/#more-19464

Andrews, R., 2017b: *Making the Measurements Match the Models – Part 2: Sea Surface Temperatures*, Energy Matters, Aug 2. http://euanmearns.com/making-the-measurements-match-the-models-part-2-sea-surface-temperatures/

Andrews, R., 2017c: *Adjusting Measurements to Match the Models – Part 1: Surface Air Temperatures*, Energy Matters, July 27. http://euanmearns.com/adjusting-measurements-to-match-the-models-part-1-surface-air-temperatures/

Argo, 2021: *Global Argo Marine Atlas*. https://argo.ucsd.edu/data/data-visualizations/marine-atlas/

Arrhenius, S., 1896: *On the influence of carbonic acid in the air upon the temperature of the ground*, The London, Edinburgh, and Dublin Philosophical Magazine and Journal of Science, v. 41, pp. 237-276. https://doi.org/10.1080/14786449608620846

Bryson, R. A. and G. J. Dittberner, 1976: *A non-equilibrium model of hemispheric mean surface temperature*, J. Atmos. Sci., v. 33, no. 11, pp. 2094-2106. https://journals.ametsoc.org/view/journals/atsc/33/11/1520-0469_1976_033_2094_anemoh_2_0_co_2.xml

Callendar, G. S., 1938: *The artificial production of carbon dioxide and its influence on temperature*, J. Roy. Met. Soc., v. 64, pp. 223-240. https://doi.org/10.1002/qj.49706427503 Available at: http://www.met.reading.ac.uk/~ed/callendar_1938.pdf

Clark, R., 2013a: *A dynamic, coupled thermal reservoir approach to atmospheric energy transfer Part I: Concepts,* Energy and Environment, v. 24, nos. 3-4, pp. 319-340. https://doi.org/10.1260/0958-305X.24.3-4.319

Clark, R., 2013b: *A dynamic, coupled thermal reservoir approach to atmospheric energy transfer Part II: Applications*, Energy and Environment, v. 24, nos. 3-4 pp. 341-359. https://doi.org/10.1260/0958-305X.24.3-4.341

Clark, R., 1993, *Optical measurement with direct traceability to the primary standards of length and time: toward a system of metrology based entirely on the properties of the photon*, Optical Engineering, v. 32, no. 3, pp. 571-584. [https://doi.org/10.1117/12.61045]

Clark, R. and A. Rörsch, 2023: *Finding Simplicity in a Complex World - The Role of the Diurnal Temperature Cycle in Climate Energy Transfer and Climate Change*, Clark Rörsch Publications, Thousand Oaks, CA. https://clarkrorschpublication.com/

D'Aleo J. and A. Watts, 2010: *Surface temperature records: policy driven deception?* Aug. 27, http://scienceandpublicpolicy.org/images/stories/papers/originals/surface_temp.pdf (Link not working) Available at: https://venturaphotonics.com/files/6.0_D'Aaleo.Watts.Surface_temp.SPPC%202010.pdf

Douglas, J. H., 1975: *Climate change: chilling possibilities*, Science News, March 1, v. 107, pp.

138-140. https://www.sciencenews.org/wp-content/uploads/2008/10/8983.pdf

Fourier, J.-B. J., 1824: *Remarques générales sur les températures du globe terrestre et des espaces planétaires*, Annales de Chimie et de Physique, v, 27, pp. 136–167. https://gallica.bnf.fr/ark:/12148/bpt6k65708960/f142.image# English translation: http://fourier1824.geologist-1011.mobi/

Fourier, J.-B. J., 1827: *Mémoire sur les températures du globe terrestre et des espaces planétaires*, Mém. Acad. R. Sci. Inst. Fr., v. 7, pp. 527-604. https://www.academie-sciences.fr/pdf/dossiers/Fourier/Fourier_pdf/Mem1827_p569_604.pdf English translation: http://www.wmconnolley.org.uk/sci/fourier_1827/

Fourier, J. -B. J., 1822: *Theorie Analytique de la Chaleur*, Didot, Paris. https://gallica.bnf.fr/ark:/12148/bpt6k29061r/f7.item

Gray, S. T., L. J. Graumlich, J. L. Betancourt and G. T. Pederson, 2004: *A tree-ring based reconstruction of the Atlantic Multi-decadal Oscillation since 1567 A.D.*, Geophys. Res. Letts., v. 31, L12205, pp. 1-4. https://doi.org/10.1029/2004GL019932

Gray, S. T., L. J. Graumlich, J. L. Betancourt and G. T. Pederson, 2004: *Atlantic Multi-decadal Oscillation (AMO) Index Reconstruction,* IGBP PAGES/World Data, Center for Paleoclimatology, Data Contribution Series #2004-062, NOAA/NGDC Paleoclimatology Program, Boulder CO, USA. https://www.ncei.noaa.gov/pub/data/paleo/treering/reconstructions/amo-gray2004.txt

HadCRUT4, 2022: *HadCRUT4 Data Series*, https://www.metoffice.gov.uk/hadobs/hadcrut4/data/current/time_series/HadCRUT.4.6.0.0.annual_ns_avg.txt

Hale, G. M. and M. R. Querry, 1973: *Optical constants of water in the 200 nm to 200 μm wavelength region*, Applied Optics, v. 12, no. 3, pp. 555-563. https://doi.org/10.1364/AO.12.000555

Hansen, J., D. Johnson, A. Lacis, S. Lebedeff, P. Lee, D. Rind and G. Russell, 1981: *Climate impact of increasing carbon dioxide*, Science, v. 213, pp. 957-956. https://pubs.giss.nasa.gov/docs/1981/1981_Hansen_ha04600x.pdf

IPCC AR6, 2021: Forster, P., T. Storelvmo, K. Armour, W. Collins, J.-L. Dufresne, D. Frame, D.J. Lunt, T. Mauritsen, M.D. Palmer, M. Watanabe, M. Wild, and H. Zhang, *The Earth's Energy Budget, Climate Feedbacks, and Climate Sensitivity*. In: Masson-Delmotte, V., P. Zhai, A. Pirani, S.L. Connors, C. Péan, S. Berger, N. Caud, Y. Chen, L. Goldfarb, M.I. Gomis, M. Huang, K. Leitzell, E. Lonnoy, J.B.R. Matthews, T.K. Maycock, T. Waterfield, O. Yelekçi, R. Yu, and B. Zhou (eds.), *Climate Change 2021: The Physical Science Basis*. *Contribution of Working Group I to the Sixth Assessment Report of the Intergovernmental Panel on Climate Change*. Cambridge University Press, Cambridge, United Kingdom and New York, NY, USA. Chapter 7, pp. 923-1054. doi: 10.1017/9781009157896.009, https://www.ipcc.ch/report/ar6/wg1/

IPCC FAR, (1990), Houghton, J. T., G. J. Jenkins and J. J. Ephraums (Eds.), *Climate Change, The IPCC Scientific Assessment*, Cambridge University Press, New York. [https://www.ipcc.ch/site/assets/uploads/2018/03/ipcc_far_wg_I_full_report.pdf]

Jones, P. D., T. M. L. Wigley, C. K. Foland, D. E. Parker, J. K. Angell, S. Lebedeff and J. E. Hansen, 1988: *Evidence for global warming in the past decade*, Nature, v. 332, p. 790. https://doi.org/10.1038/332790b0

Jones, P. D., T. M. Wigley and P. B Wright, 1986: *Global temperature variations between 1861 and 1984*, Nature, v. 323 no.31, pp. 430-434. https://www.nature.com/articles/322430a0

Keeling, 2023: *The Keeling Curve*. https://scripps.ucsd.edu/programs/keelingcurve/

Kirchoff, G., (1860), *On the relation between the radiating and absorbing powers of different bodies for light and heat*, Philosophical Magazine Series 4, v. 20 pp. 1-21, (Translation by F.

Guthrie) https://archive.org/details/londonedinburghd20lond/page/n15

Original publication: *Ueber das Verhältniss zwischen dem Emissionsvermögen und dem Absorptionsvermögen der Körper für Wärme en Licht*, Annalen der Physik en Chemie, v. 109 no. 2 pp. 275-301. http://www.bio-physics.at/wiki/images/Kirchhoff_Emissions_und_Absorptions-vermoegen.pdf

Knutti, R. and G. C. Hegerl, 2008: *The equilibrium sensitivity of the Earth's temperature to radiation changes*, Nature Geoscience, v. 1 pp. 735-743. https://www.nature.com/articles/ngeo337

Lettau, H. H. and B. Davidson (1957), *Exploring the Atmosphere's First Mile. Proceedings of the Great Plains Turbulence Field Program, 1 August to 8 September 1953* Volume II, Site Description and Data Tabulation, Oxford, Pergamon Press.

Available at:
https://books.google.com/books?hl=en&lr=&id=5bcJAQAAIAAJ&oi=fnd&pg=PA377&dq=Lettau,+H.H.+and+B.+Davidson,+Exploring+the+atmosphere%E2%80%99s+first+mile.+Oxford:+Pergamon+Press,+1957.&ots=N0vbpjURx3&sig=sSTz9EMWpwi0XysXHTcWcLNxWv0#v=onepage&q&f=false

Manabe, S. and R. T. Wetherald, 1967: *Thermal equilibrium of the atmosphere with a given distribution of relative humidity*, J. Atmos. Sci., v. 24 pp. 241-249. http://www.gfdl.noaa.gov/bibliography/related_files/sm6701.pdf

McFarlane, F., 2018: *The 1970s Global Cooling Consensus was not a Myth*, Watts Up with That, Nov. 19. https://wattsupwiththat.com/2018/11/19/the-1970s-global-cooling-consensus-was-not-a-myth/

Morice, C. P., J. J. Kennedy,N. A. Rayner and P. D. Jones, 2012: *Quantifying uncertainties in global and regional temperature change using an ensemble of observational estimates: The HadCRUT4 data set*, J. Geophysical Res. Atmospheres, v. 117, D08101, pp. 1-22. https://doi.org/10.1029/2011JD017187

Oke T. R., 2006: *Initial guidance to obtain representative meteorological observations at urban sites*, Instruments and Observing Methods, Report No. 81, WMO/TD-No. 1250, World Meteorological Association, pp. 47.

https://www.researchgate.net/publication/265347633_Initial_guidance_to_obtain_representative_meteorological_observations_at_urban_sites

Ollila, A., 2023: *Natural Climate Drivers Dominate in the Current Warming*, Science of Climate Change, v. 3, no.3, pp. 290-326. https://doi.org/10.53234/scc202304/03

Peterson, T. C., W. M. Connolley and J. Fleck, 2008: *The myth of the 1970's global cooling consensus*, Bull. Amer. Meteor. Soc., v. 86, pp. 1325-1337. [https://doi.org/10.1175/2008BAMS2370.1]

Pouillet, M., 1837: *Memoir on the solar heat, on the radiating and absorbing powers of the atmospheric air and on the temperature of space.* In: Scientific Memoirs selected from the Transactions of Foreign Academies of Science and Learned Societies, edited by Richard Taylor, v. 4, pp. 44-90.

http://nsdl.library.cornell.edu/websites/wiki/index.php/PALE_ClassicArticles/archives/classic_articles/issue1_global_warming/n2-Poulliet_1837corrected.pdf

Original publication, 1836: *Mémoire sur la chaleur solaire: sur les pouvoirs rayonnants et absorbants de l'air atmosphérique et sur la température de l'espace,* Comptes Rendus des Séances de l'Académie des Sciences, Paris. v. 7, pp. 24-65.

Ramaswamy, V., W. Collins, J. Haywood, J. Lean, N. Mahowald, G. Myhre, V. Naik, K. P.

Shine, B. Soden, G. Stenchikov and T. Storelvmo, 2019: *Radiative Forcing of Climate: The Historical Evolution of the Radiative Forcing Concept, the Forcing Agents and their Quantification, and Applications* Meteorological Monographs v. 59, Chapter 14. https://doi.org/10.1175/AMSMONOGRAPHS-D-19-0001.1

TRITON, 2021: *TRITON Buoy Data*. https://www.pmel.noaa.gov/tao/drupal/disdel/

WRCC, 2021: *Western Region Climate Center*. https://wrcc.dri.edu/sod/arch/hbF.html